

Charging Scheduling of Electric Vehicle Incorporating Grid-to-Vehicle and Vehicle-to-Grid Technology Considering in Smart Grid

Sourav Das[✉], Student Member, IEEE, Parimal Acharjee, Senior Member, IEEE,
and Aniruddha Bhattacharya, Member, IEEE

Abstract—In recent days, the deployment of electric vehicles (EVs) in automobile sector is increasing the load demand in the distribution system. To deal with this load demand, the charging management needs to be improved. Nevertheless, an EV needs several hours to complete charge. Reducing the charging time, energy consumption is a huge contest to deal with the promotion of EV over conventional vehicles. The condition of the itineraries may affect the energy consumption of the EV, which needs to be considered before fulfilling the energy demand. In this article, these are considered assigning suitable charging stations (CS) to individual EVs and their scheduling is taken as an optimization problem. The first part deals with the proper assignment of CS, which is a linear optimization problem and the second deals with the charging scheduling problem. An “intelligent charging scheduling algorithm (ICSA)” is proposed with the integration of Henry gas solubility optimization to minimize total daily price incurred by the CS operator. Later, ICSA is clubbed with other standard optimization techniques considering practical constraints. A 2 m point estimation method has been utilized to tackle the uncertainty and its performance has been compared with the Monte-Carlo simulation technique. The robustness of ICSA is evaluated and confirmed using the Wilcoxon signed rank test and Quade test.

Index Terms—Charging stations (CS), distribution system, electric vehicle (EV), Monte Carlo simulation (MCS), optimizations, scheduling, 2 m point estimation method (2m-PEM).

NOMENCLATURE

Abbreviations

CS	Charging stations.
CSO	Charging station operator.
EV	Electric vehicles.
EVSE	Electric vehicle supply equipment.
FFPV	Fossil fuel powered vehicles.

Manuscript received April 9, 2020; revised June 27, 2020 and September 10, 2020; accepted November 1, 2020. Date of publication December 1, 2020; date of current version March 17, 2021. Paper 2020-SECSC-0520.R2, presented at the 2020 IEEE International Conference on Power Electronics, Smart Grid and Renewable Energy, Cochin, India, Jan. 2–4, and approved for publication in the IEEE TRANSACTIONS ON INDUSTRY APPLICATIONS by the Renewable and Sustainable Energy Conversion Systems Committee of the IEEE Industry Applications Society. (*Corresponding author: Sourav Das.*)

The authors are with the Department of Electrical Engineering, National Institute of Technology, Durgapur, Durgapur 713209, India (e-mail: svdas111@gmail.com; parimal.acharjee@gmail.com; aniruddha.bhattacharya@ee.nitdgp.ac.in).

Color versions of one or more of the figures in this article are available online at <https://ieeexplore.ieee.org>.

Digital Object Identifier 10.1109/TIA.2020.3041808

G2V	Grid to vehicle.
HBC	Higher battery capacity.
HGSO	Henry gas solubility optimization.
ICSA	Intelligent charging scheduling algorithm.
ILPP	Integer linear programming problem.
IRV	Input random variable.
MCS	Monte Carlo simulation.
PEM	Point estimation method.
ORV	Output random variable.
PEV	Plug-in electric vehicles.
PHEV	Plug-in hybrid electric vehicles.
QT	Quade test.
RTT	Real-time tariff.
SOC	State of charge.
V2G	Vehicle to grid.
WSRT	Wilcoxon signed ranked test.

Parameters

AER	All electric range.
ch _{rate,PEV_no} _{min}	Minimum charging rate of EVs.
ch _{rate,PEV_no} _{max}	Maximum charging rate of EVs.
De	Demand of vehicles for CS.
DOD	Battery's depth of discharge.
ETL	Ensuing trip length.
L^{batt}	Batteries lifecycle at fixed DOD.
PW _{rated}	Charger's power ratings in the CS.
S	Availability of charging slots.
SOC ^{min}	Minimum SOC of the battery.
SOC ^{max}	Maximum SOC of the battery.
η^{ch}	Charging efficiency of the vehicle.
η^{dis}	Discharging efficiency of the vehicle.

Indices

e	Number of vehicles needs charge.
f	Total number of CS.
t	Time needed to reach the CS.
k	Jam coefficient constant.
m	Number of uncertain IRV.
no	EV's index arriving at CS in 30 min time interval.
N	Number of observations.
pos	Location for IRV z_l .

PEV_no	Index of EVs at 30 min interval arriving to the CS.	SOC^{req}	Required SOC by each EV in the parking duration.
slot	Time index at 30 min time interval.	SOC_{ini}	Initial SOC of individual EV before reaching to the CS.
tot.PEV	Number of EVs coming to the CS in 24 h.	slot_in	Arrival slots of individual EV at CS.
y	Location of ORV.	slot.out	Departure slots of individual EV at CS.
<i>Variables</i>		ST_{PEV_no}	Strategy vector of PEV_no th number of EV ($PEV_no \in \vec{Z}$).
$Batt^{cap,PEV_no}; b_{cap}$	Individual vehicles battery capacity.	$ST_{PEV_no}^{slot}$	Charging strategy vector's value of PEV_no number of EV time at interval index "slot" ($PEV_no \in \vec{Z}$).
$batt_{cost,PEV_no}$	Cost of the battery of EVs.	$ST_{PEV_no}^{slot_in}$	Value of charging strategy of PEV_no th number EV at arrival time interval "slot_in" ($PEV_no \in \vec{Z}$).
$Cost^{TOT}$	Total daily price incurred by CSO for tot.PEV EVs.	$ST_{PEV_no}^{slot_out}$	Value of charging strategy of PEV_no th number EV at departure time interval "slot_out" ($PEV_no \in \vec{Z}$).
$Cost^{och}$	Overall cost for complete charging process for tot.PEV EVs.	$SOC_{PEV_no}^{slot}$	State of charge of PEV_no th vehicle at time index "slot" ($PEV_no \in \vec{Z}$).
$Cost_{batt.deg}$	Degradation cost of batteries for tot.PEV EVs.	T	Complete time duration vector in 24 h.
$Cost^{G2V}$	Cost due to G2V mode for tot.PEV EVs.	$t_{in,PEV_no}/t^{arr}$	Time of PEV_no th EV arriving at CS.
$Cost^{V2G}$	Earn due to V2G mode tot.PEV EVs.	$t_{out,PEV_no}/t^{dep}$	Time of PEV_no th EV departing from CS.
$ch^{rate,PEV_no/ch}$	Required charging rates for PEV_no th ($PEV_no \in \vec{Z}$).	$v(f, e, t)$	eth vehicle's speed to fth CS at time t.
C_{PEV_no}	Vector for charging strategy of PEV.no th EV ($PEV_no \in \vec{Z}$).	$v_q(f, e, t)$	Vehicles flow between eth vehicle and fth CS at time t.
$C_{PEV_no}^{slot}$	The value of C_{PEV_no} in the time interval "slot" ($PEV_no \in \vec{Z}$).	$W_{l, pos}$	Weighting factor, which specifies the dominance of the conforming location (pos = 1, 2).
$Cost_{lab}$	Labor cost of the battery of EVs.	x	Decision variable (1 or 0) to identify the CS for individual EVs.
D	Daily mileage of EVs.	\vec{Z}	Number of cars arriving in a CS.
DC_{PEV_no}	Vector for discharging strategy of PEV_no th EV ($PEV_no \in \vec{Z}$).	$Z_{l, pos}$	Estimated location for IRV at pos = 1, 2.
$DC_{PEV_no}^{slot}$	The value of DC_{PEV_no} in the time interval "slot" ($PEV_no \in \vec{Z}$).	μ_{zl}	Average value of IRV Zl .
$dch^{rate,PEV_no/dch}$	Required discharging rates for PEV_no th EVs ($PEV_no \in \vec{Z}$). $d(f, e, t)/dis^{e-f}$ Distance of f th CS of eth vehicle at time t.	σ_{zl}	Standard deviation for IRV Zl .
d^f	First trip distance of individual EVs.	$\lambda_{Zl,3}$	Skewness of IRV Zl .
E	The value of expectations.	$\lambda_{Zl,4}$	Kurtosis of IRV Zl .
Eng^{dis}	Total energy discharge due to V2G from individual EVs.	$\xi_{Zl, pos}$	Standard location for IRV at pos = 1, 2.
E^{con}	Energy consumption while reaching the CS by EVs.	μ_c	Average value of ORV.
Eng^{req}	Total energy drawn due to G2V for individual EVs.	σ_C	Standard value of ORV.
\vec{H}	Vector for time horizon.		
$j_{jam}(f, e, t)$	Traffic density between fth CS and eth EV at time t.		
L^{batt}	Lifecycle of the EV's battery at particular DOD.		
P_{slots,PEV_no}	Parking duration for PEV_no th EV ($PEV_no \in \vec{Z}$).		
$Prob(Z_{l,j})$	Probability of individual IRV $Z_{l,j}$.		
Pw_{PEV}^{slots}	Total power requirement by all the vehicles.		
$RTT(slot)$	Value of RTT per slot.		
SOC^{arr}	Individual EV's arrival SOC while arriving at CS.		
SOC^{dep}	Individual EV's departure SOC while departing at CS.		

I. INTRODUCTION

IN THIS age of globalization, the usage of internal combustion (IC) engine vehicles has a massive negative impact on the environment. The problems with fossil fuel powered vehicles (FFPV) are as follows.

- 1) Fossil fuels are a scarce resource.
- 2) Spilling of oil may be hazardous.
- 3) It is very expensive nowadays.

Therefore, in recent days, due to the cheaper rate of electricity and zero pollution features, EVs are grabbing attention. EVs are much more reliable and require less maintenance than FFPVs. EV has quiet and smooth driving features. Among various types of EVs, people are in specific tending toward PEV, as it is more reliable and efficient than pure EVs.

A huge deployment of EVs needs a good charging infrastructure so that it may able to meet the charging demands of EVs smoothly and smartly. Intelligent charging management and scheduling are the two key solutions to such a problem.

At a very initial stage, a simple scheduling has been performed by considering various driving cycle attributes, such as arrival time, departure time, daily mileage, and first trip distance, as shown in [1], where the attributes are deterministic in nature. Researchers are, nowadays, focusing more to improve these factors to make this better. But every new technology has its own cons with which the researchers have to deal with. Every time, EV drivers face the anxiety about “when” and “where” to charge their vehicles. Therefore, it is important to identify the “appropriate” charging station (CS). To deal with this scenario, many researchers have proposed various methods. But most of them have considered the distance as the only feature to identify the adequate CS for corresponding vehicles [2].

In [3]–[5], Wu *et al.* have proposed a quick charging solution by increasing the charging current and voltage. Few of them used ultracapacitors also to reduce the charging time and named those as apt CS [6]. But, to identify an adequate CS, the availability of free charging slots in CS is the most important factor, which needs to be considered. Therefore, this factor is incorporated in this article along with other factors, such as less battery energy consumption and shortest distance, to identify an adequate CS.

After the allotment of relevant CS to the corresponding vehicles, charging scheduling is the next key challenge to deal with. Moreover, managing EV charging in an optimal way is always a great challenge. Many authors are focused on the methodology of EV charging using the G2V mode. How the surplus energy of the EV can be utilized for the betterment of the grid is another major concern and this introduces a new era in EV smart charging technology, termed as V2G technology. For the charging scheduling purpose, some authors have proposed a window optimization technique, which is suitable for online application due to its incessant update of the information pattern. This determined the optimal scheduling with minimal charging cost [7].

In [8], considering various driving patterns, it has been shown that due to high pricing during the day time and offering less tariff at night, EV owners are provoked to charge the EVs during the night. In the literature [9], an energy management scenario has been established considering three types of traffic conditions, with the main objective to increase the fuel economy of PEV by integrated traffic information.

In [10], an autonomous distributed V2G control scheme has been used, where EV can be utilized as spinning reserves for the grid. In [11], the proposed charging strategy is allowing EVs to operate either in the V2G mode or in G2V mode while in the CS.

The major limitation with these articles is, PEV has been operated either in the G2V mode or in the V2G mode, while in CS in a particular time. Few of them operated PEV in the G2V mode continuously for a certain duration and also again in the V2G mode continuously for a certain duration, where frequent switching between the G2V mode and V2G mode is missing [10]–[13].

But in this article, it has been shown that the proposed algorithm can handle both between G2V and V2G modes of operation after a certain interval (atleast 30 min), in an efficient manner, which is different from the earlier concepts adopted by the previous articles, which may result in a profitable scenario for both CSO and the EV owner.

Again, in [12], fixed charging rates have been considered, which are not economical for CSOs, as the electricity price may vary due to the grid’s generation and demands mismatch, which makes the electricity tariff dynamic. Therefore, in this article, dynamic charging rates have been used so that CSO can control and vary the charging rates as per the RTT at different intervals, and consequentially, the operation can be economical.

From the critical literature survey [15]–[17], it has been observed that in these articles, fix data of driving cycles have been used to perform the charging scheduling. But these attributes are always uncertain in nature. Therefore, fluctuations of values may be possible in these attributes, which are very critical and need to be considered to perform better charging scheduling. Hence, in this article, the uncertainty related to driving cycles has been handled using 2m-PEM.

Previous articles have not considered 2m-PEM in order to handle the probabilistic driving pattern. Different probabilistic methods, such as MCS, approximate methods [18], truncated Taylor series expansion method [19], and the discretization method [20], are there, which have some major limitations while handling a large number of uncertain variables. Scientist H. P. Hong developed an efficient and modified 2m-PEM method for probabilistic analysis, which is computationally moderate and has the ability to deal with a large number of uncertainties in less time [21]. It uses deterministic routines to handle the stochastic frameworks and also has less computational complexity and is efficient enough to handle a large number of uncertainties. One more advantage is that, at the end of the optimization problem, the best solution set, which is obtained, represents the mean value of the objective function and not the actual value of the objective function. The mean value is used since the present problem deals with a large number of uncertain variables. Hence, it is always better to use the mean value than the best value while dealing with the randomness of uncertain variables related to the driving cycle.

The proposed ICSA can be divided into two major parts. The first part of ICSA deals with the building up of mathematical problem formulations for selecting the “appropriate” CS, dealing with the uncertainties related to driving cycles by applying 2m-PEM, and combined charging scheduling of the EVs, whereas the second part of the ICSA, tackles the minimization of the total daily price incurred by CSO, by appropriately clubbing various optimization techniques.

The key contributions of this article are as follows.

- 1) Appropriate CS has been selected with respect to the consumption of battery energy required to reach that very CS and the availability of the slots.
- 2) Both G2V and V2G modes of operation after a certain interval have been considered and handled by the proposed ICSA.

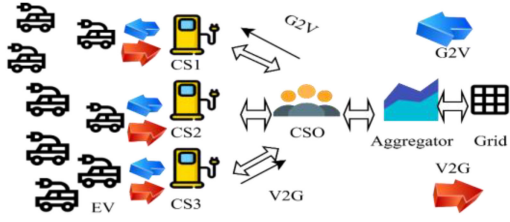


Fig. 1. Basic diagram for problem definition.

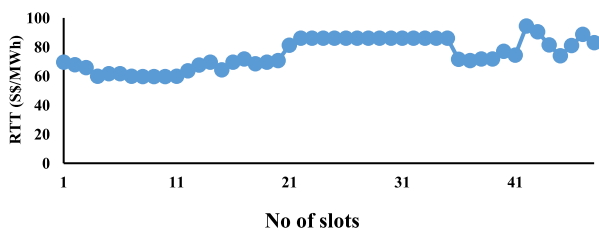


Fig. 2. RTT from NEMS.

- 3) While performing the scheduling, variable charging rates have been considered since it is more economical than fixed charging rates.
- 4) Various uncertain attributes of driving cycles used in ICSA are stochastic in nature and have been critically handled by 2m-PEM. The performance of 2m-PEM has been compared with the conventional MCS method.

II. PROBLEM FORMULATION FOR ICSA

A. Problem Positioning

The main anxiety works on EV drivers are “where” and “when” they can charge their EV at the minimum queue in a suitable CS. A CS can be said suitable when there will be free charging points available, which will provide the service immediately after reaching. It must be located near some centers of interest and one must be able to reach with the minimum traffic congestions with less energy consumptions. It is notable that by considering all the above-mentioned criteria, it is not necessary that the nearest CS will be the most suitable one. Fig. 1 shows the overall diagram for the problem definition.

Now upon the arrival of the corresponding vehicle to their respective CS, SOC_{arr} , t_{arr} , t_{dep} , ETL, and type of vehicles [b_{cap} and all electric range (AER)] need to be provided to the CSO.

Considering these factors, the required energy has been evaluated for every EVs. Now, as per t_{arr} and t_{dep} , the optimal scheduling has been executed by taking into consideration the G2V mode and V2G mode to satisfy the required energy.

B. Objective Function Formulation

The main objective of this scheduling is to minimize the total daily price incurred by CSO, which has been shown as follows:

$$\min \{Cost^{\text{TOT}}\}. \quad (1)$$

This contains two major parts, such as $(Cost^{\text{oCh}})$ and $(Cost_{\text{batt.deg}})$ as shown

$$Cost^{\text{TOT}} = Cost^{\text{oCh}} \cup Cost_{\text{batt.deg}}. \quad (2)$$

Again, the $Cost^{\text{oCh}}$ is the resultant of $Cost^{\text{G2V}}$ and $Cost^{\text{V2G}}$, i.e.,

$$\begin{aligned} Cost^{\text{oCh}} &= (Cost^{\text{G2V}} + (-Cost^{\text{V2G}})) \text{ or} \\ Cost^{\text{oCh}} &= Cost^{\text{G2V}} \cup Cost^{\text{V2G}}. \end{aligned} \quad (3)$$

Now, in order to calculate these $Cost^{\text{G2V}}$, $Cost^{\text{V2G}}$, and $Cost_{\text{batt.deg}}$ [20], the corresponding formulae have been shown

$$Cost^{\text{G2V}} = \sum_{\text{slot}=1}^{\text{tot_slot}} \left(\sum_{\text{PEV_no}=1}^{\text{tot_PEV}} (C_{\text{PEV_no}}^{\text{slot}}) (ch^{\text{rate,PEV_no}}) \right) RTT(\text{slot}) \quad (4)$$

$$Cost^{\text{V2G}}$$

$$= \sum_{\text{slot}=1}^{\text{tot_slot}} \left(\sum_{\text{no}=1}^{\text{tot_PEV}} (DC_{\text{PEV_no}}^{\text{slot}}) (dch^{\text{rate,PEV_no}}) * RTT(\text{slot}) \right) \quad (5)$$

$$\begin{aligned} Cost_{\text{batt.deg}} &= \sum_{\text{PEV_no}=1}^{\text{tot_PEV}} \\ &\times \left(\frac{(batt_{\text{cost,PEV_no}} * Batt^{\text{cap,PEV_no}} + Cost_{\text{lab}}) * |Eng^{\text{dis}}|}{(L^{\text{batt}} * Batt^{\text{cap,PEV_no}} * DOD)} \right). \end{aligned} \quad (6)$$

C. Constraints in ICSA

While executing ICSA, few practical constraints need to be considered, i.e., subjects to the charging rates, the battery SOC, and the fulfillment of energy requirements. These need to be considered while scheduling for the real-time feasibility.

1) Charging Rates:

$$ch^{\text{rate,PEV_no}} < PW_{\text{rated}} \quad (7)$$

$$ch^{\text{rate,PEV_no}}_{\text{min}} \leq ch^{\text{rate,PEV_no}} \leq ch^{\text{rate,PEV_no}}_{\text{max}}. \quad (8)$$

The charging or discharging rate should not surpass the charging slot's power ratings, as shown in (7). The charge controller can vary its charging rate or discharging rate in between its rated capacity, as shown in (8).

2) Energy Requirements:

$$\sum_{\text{slot}=\text{slot}_{\text{in}}}^{\text{slot}_{\text{out}}} ST_{\text{PEV_no}}^{\text{slot}} \cdot ch^{\text{rate,PEV_no}} = Eng^{\text{req}}. \quad (9)$$

It must be satisfied within the parking time duration with dynamic charging and discharging rates controlled by CSO.

3) Battery SOC:

$$SOC^{\text{min}} \leq SOC_{\text{PEV_no}}^{\text{slot}} \leq SOC^{\text{max}}. \quad (10)$$

The battery SOC should not surpass or go underneath its minimum and maximum level, which is 20% and 90%, respectively.

4) *Number of CS*: The number of CS is very less than the number of vehicles.

D. Charging and Discharging Strategy

In (11) and (13), to determine the charging and discharging strategy, (12) and (14) have been developed

$$C_{\text{PEV_no}} = \left[C_{\text{PEV_no}}^1, \dots, C_{\text{PEV_no}}^{\text{slot_in}}, \dots, C_{\text{PEV_no}}^{\text{slot_out}}, \dots, C_{\text{PEV_no}}^{\text{tot_slot}} \right] \quad (11)$$

where

$$C_{\text{PEV_no}}^{\text{slot}} = \begin{cases} 1, & \text{if } ST_{\text{PEV_no}}^{\text{slot}} = 1, \forall \text{ slot : } P_{\text{slots,PEV_no}}, \\ & \forall \text{PEV_no} \in \vec{Z} \\ 0, & \text{or else} \\ 0, & \forall \text{ slot } \notin P_{\text{slots,PEV_no}}, \\ & \forall \text{PEV_no} \in \vec{Z} \end{cases} \quad (12)$$

$$DC_{\text{PEV_no}} = \left[DC_{\text{PEV_no}}^1, \dots, DC_{\text{PEV_no}}^{\text{slot_in}}, \dots, DC_{\text{PEV_no}}^{\text{slot_out}}, \dots, DC_{\text{PEV_no}}^{\text{tot_slot}} \right] \quad (13)$$

where

$$DC_{\text{PEV_no}}^{\text{slot}} = \begin{cases} -1, & \text{if } ST_{\text{PEV_no}}^{\text{slot}} = -1 \forall \text{ slot : } \\ & P_{\text{slots,PEV_no}} \forall \text{PEV_no} \in \vec{Z} \\ 0, & \text{or else} \\ 0, & \forall \text{ slot } \notin P_{\text{slots,PEV_no}}, \forall \text{PEV_no} \in \vec{Z} \end{cases} \quad (14)$$

The charging strategy for PEV_{no}th vehicle can be defined by

$$ST_{\text{PEV_no}} = \left[ST_{\text{PEV_no}}^1, ST_{\text{PEV_no}}^{\text{slot_in}}, \dots, ST_{\text{PEV_no}}^{\text{slot}}, \dots, ST_{\text{PEV_no}}^{\text{slot_out}}, \dots, ST_{\text{PEV_no}}^{\text{tot_slot}} \right] \quad (15)$$

where

$$ST_{\text{PEV_no}}^{\text{slot}} = \begin{cases} 1, & \text{charging} \\ -1, & \text{discharging}, \forall \text{PEV_no} \in \vec{Z} \\ 0, & \text{idle} \end{cases} \quad (16)$$

where the strategy should be such that

$$\sum_{\text{slot}=\text{slot_in}}^{\text{slot_out}} ST_{\text{PEV_no}}^{\text{slot}} \cdot ch^{\text{rate}} = Eng^{\text{req}}, \quad \forall \text{PEV_no} \in \vec{Z}. \quad (17)$$

Energy discharged and power requirements by all the vehicles can be formulated as

$$Eng^{\text{dis_no}} = \sum_{\text{slot}=1}^{\text{tot_slot}} DC_{\text{PEV_no}}^{\text{slot}} * ch^{\text{rate,PEV_no}} \forall \text{PEV_no} \in \vec{Z} \quad (18)$$

$$Pw_{\text{PEV}}^{\text{slots}} = \sum_{\text{PEV_no}=1}^{\text{tot_PEV}} (C_{\text{PEV_no}}^{\text{slot}} - DC_{\text{PEV_no}}^{\text{slot}}) ch^{\text{rate,PEV_no}} \quad \forall \text{ slots} \in \vec{H}. \quad (19)$$

Again, the parking duration for PEV_{no}th is given by

$$P_{\text{slots,PEV}} = [t_{\text{in,PEV_no}}, \dots, t_{\text{PEV_no}}, \dots, t_{\text{out,PEV_no}}]. \quad (20)$$

Since it is 24 h scheduling, therefore, it has been divided into 48 slots of half hours each.

The charging coordination of EVs (e.g., every 30 min) to minimize the total daily price incurred by CSO by integrating the G2V mode and V2G mode needs to be executed, where the time horizon vector is given by \vec{H}

$$\vec{H} = [1, \dots, \text{slot}, \dots, \text{tot_slot}]. \quad (21)$$

The number of cars arriving in a CS is denoted by the vector

$$\vec{Z} = [1, \dots, \text{PEV_no}, \dots, \text{tot_PEV}]. \quad (22)$$

When PEVs are plugged in, three possible operations, i.e., charging (+1), discharging (-1), and idle (0), will occur in order to satisfy eng^{req}.

E. Energy Modeling

In order to satisfy the constraints given in (9), the energy modeling is given by

$$eng^{\text{req}} = \frac{SOC^{\text{req}} \cdot b_{\text{cap}}}{\eta^{\text{ch}}} \quad (23)$$

$$eng_{\text{dis}}^{\text{req}} = SOC^{\text{req}} \cdot b_{\text{cap}} \cdot \eta^{\text{dis}}. \quad (24)$$

Now, again to calculate SOC^{req}, the following equation is given:

$$SOC^{\text{req}} = \begin{cases} 1 - SOC^{\text{arr}}, & \text{when } SOC^{\text{dep}} > 1 \\ (SOC^{\text{dep}} - SOC^{\text{arr}}), & \text{when } SOC^{\text{arr}} < SOC^{\text{dep}} < 1 \\ 0, & \text{when } SOC^{\text{arr}} = SOC^{\text{dep}} \\ -(SOC^{\text{arr}} - SOC^{\text{dep}}), & \text{when } 0.2 < SOC^{\text{dep}} < SOC^{\text{arr}} \end{cases} \quad (25)$$

where SOC^{arr} [21] and SOC^{dep} [21] can be calculated from the following:

$$SOC^{\text{arr}} = 1 - (d^f / AER) \quad (26)$$

$$SOC^{\text{dep}} = [(ETL/AER) + 20\%]. \quad (27)$$

Although SOC^{arr} and SOC^{dep} have been calculated, practically, the SOC status after the arrival and the ensuing trip distance can be obtained using EVs telematics system. Moreover, since the full charging of the battery may reduce the battery life cycle [25], [26], it is avoided.

From the above-mentioned discussion, it is clear that in order to perform the scheduling, d^f , t^{arr} , t^{dep} , and D are basically needed. But all these attributes are uncertain. Due to the unavailability of historical data, the statistical analysis (2m-PEM) has been performed to handle the uncertainty and the required estimated data have been generated. The details regarding the estimation have been discussed in the following section and the details regarding the data generation have been clarified in Section V-C.

III. UNCERTAINTY MODELING TECHNIQUE

A. Hong's 2m-PEM

To deal with the uncertainties, two deterministic points have been estimated from one probabilistic point. For one probabilistic input random variable (IRV) set, two deterministic sets of data can be achieved using 2m-PEM.

Mathematically, the deterministic agenda of the charging cost minimization problem can be represented as

$$C = \text{fn}(r_i). \quad (28)$$

The function fn transfers the uncertainty from IRVs to output variables

$$C = \text{fn}(C_r, Z_1, Z_2, \dots, Z_m) \quad (29)$$

where $Z_l (l = 1, 2, \dots, m)$ are the input variables under vagueness with the probability function fn_{Z_m} .

The statistical moment's output of IRVs has been determined using μ_{z_l} , σ_{z_l} , $\lambda_{Zl,3}$, and $\lambda_{Zl,4}$. The 2m-PEM generates two deterministic concentrations for each IRV Z_l , as $(Z_{l,1}W_{l,1})$ and $(Z_{l,2}W_{l,2})$, which implies the dominance of the conforming location in the calculation of the output random variable (ORV). Here $Z_{l,\text{pos}}$ can be determined as follows:

$$Z_{l,\text{pos}} = \mu_{z_l} + \xi_{Z_{l,\text{pos}}} * \sigma_{Z_l}, \text{ pos } = 1, 2. \quad (30)$$

In (30), the pos^{th} standard location, $\xi_{Z_{l,\text{pos}}}$, can be assessed as follows:

$$\xi_{Z_{l,\text{pos}}} = \lambda_{Zl,3}/2 + (-1)^{(3-\text{pos})} \sqrt[2]{\lambda_{Zl,4} - (\sqrt{3}\lambda_{Zl,3}/2)^2}. \quad (31)$$

In (31), $\lambda_{Zl,3}$ [19] and $\lambda_{Zl,4}$ [19] of Z_l have been calculated as follows:

$$\lambda_{Zl,3} = m_3 / (\lambda_{Zl,3})^3 \quad (32)$$

where

$$m_3 = E(Z_l - \mu_{z_l})^3 = \sum_{j=1}^N (Z_l - \mu_{z_l})^3 \cdot \text{Prob}(Z_{l,j}) \quad (33)$$

$$\lambda_{Zl,4} = m_4 / (\lambda_{Zl,4})^4 \quad (34)$$

where

$$m_4 = E(Z_l - \mu_{z_l})^4 = \sum_{j=1}^N (Z_l - \mu_{z_l})^4 \cdot \text{Prob}(Z_{l,j}). \quad (35)$$

One deterministic set is kept fixed and other IRVs are considered equal to its average value in each simulation of 2m-PEM, as follows:

$$C_{(l,\text{pos})} = \text{fn}(C_r, \mu_1, \mu_2, \dots, z_{l,\text{pos}}, \dots, \mu_{Zm}) \quad (36)$$

where $\text{pos} = 1$ and 2 and $l = 1, 2, \dots, m$.

In (36), $Z_{l,1}$ and $Z_{l,2}$ are the specified locations of the IRV Z_l , and μ_{Zm} is the average value of the rest of the IRVs.

Two weighting factors of Z_l can be calculated as

$$W_{l,\text{pos}} = \frac{(-1)^{\text{pos}}}{m} \times \frac{\xi_{Z_{l,3-\text{pos}}}}{\xi_{Z_{l,1}} - \xi_{Z_{l,2}}}. \quad (37)$$

TABLE I
STRUCTURE OF ASSIGNMENT MATRIX

	EV_1	EV_2	EV_3	...	EV_e	S
$CS1$	$C(1,1,t)$	$C(1,2,t)$	$C(1,3,t)$		$C(1,e,t)$	X
$CS2$					X
....
CSf	$C(f,1,t)$	$C(f,2,t)$	$C(f,3,t)$...	$C(f,e,t)$	X
De	I	I	I	...	I	

The expectations of the ORV can be calculated as

$$E(C^y) = \sum_{l=1}^m \sum_{\text{pos}=1}^2 (W_{l,\text{pos}} \times ((C_{l,\text{pos}}))^y), \quad y = 1, 2. \quad (38)$$

Finally, the μ_c and σ_C of the ORV can be determined as follows:

$$\mu_c = E(C^1) \text{ and } \sigma_C = \sqrt{(E(C^2)) - (E(C^1))^2}. \quad (39)$$

After explaining the problem formulation in Section II and generating the data using 2m-PEM in Section III, the solution strategy to find out the appropriate CS and combined scheduling of the EVs have been performed applying two stages of ICSA in the following section.

IV. SOLUTION STRATEGY OF ICSA

A. First Level of ICSA

The main aim is to allocate each PEV to “appropriate” CS, by keeping the arrival SOC at its maximum by consuming very less amount of energy while reaching its recommended CS, where the vacant slots are available. This has been done using integer linear programming (ILP).

To formulate ILP problem (ILPP), few sets of parameters need to be defined. The assignment matrix C can be defined as $C(f, e)$ (where $e >> f$), where each EVs e can be assigned to CS_f . The assignment matrix is based on the well-known assignment problem [23] with a mixture of the transportation problem [24], as given in Table I. Since there is a dynamic behavior in the assignment matrix coefficient, therefore, instead of $C(f, e)$, it can be defined as $C(f, e, t)$, where $t \in \text{time}$.

The demand of the vehicle is to get only one charging point at only one CS; therefore, the demand is unity.

In this ILPP, the main objective is to keep the energy consumption at its lowest value, i.e.,

$$\min \left\{ \sum_{f=1}^F \sum_{e=1}^E (E^{\text{con}}(f, e, t) \cdot x(f, e, t)) \right\} \quad (40)$$

where

$$x(f, e, t) = \begin{cases} 1, & \text{if } EV_e \text{ is assigned to } CS_f \text{ at time } t \\ 0, & \text{otherwise} \end{cases} \quad (41)$$

subject to

$$\sum_{f=1}^{CS} x(f, e, t) = 1 \quad \forall EV_e \quad (42)$$

where $1 \leq e \leq \text{EV}$ and each vehicle can be assigned to only one CS at a time

$$\sum_{e=1}^{\text{ev}} x(f, e, t) \leq \text{CS}_f \forall \text{CS}_f \quad (43)$$

where $1 \leq f \leq \text{CS}$ the capacity of each CS should not exceed its limit.

The d^f should not be lower than the EV's dis^{e-f}

$$\text{dis}^{e-f} \leq d^f. \quad (44)$$

1) Energy Modeling in Linear Optimization Problem: In order to model the energy consumption in the assignment matrix, various factors, such as $(v(f, e, t))$, $(d(f, e, t))$, AER(e), its $(b_{\text{cap}}(e))$, $(v_q(f, e, t))$, and $(j_{\text{jam}}(f, e, t))$, have been considered [25].

The required time for covering the distance $(d(f, e, t))$ by the EV can be expressed as

$$T = d/v, \text{ where } T, d, v : \text{fn}(f, e, t). \quad (45)$$

Again, from the equation of Greenshields model [27], it has been proved that v_q is directly proportional to the j_{jam}

$$v_q \propto j_{\text{jam}} \quad (46)$$

$$\text{or } v_q = k \cdot j_{\text{jam}} \quad (47)$$

where $k = \frac{1}{v}$ and $v_q, j_{\text{jam}} \in \text{fn}(f, e, t)$.

The consumed energy E_{con} [2] under normal conditions is

$$E_{\text{con}} = \frac{b_{\text{cap}} \cdot d}{\text{AER}} \quad (48)$$

where $\text{AER} \in \text{fn}(e)$ and $d \in \text{fn}(f, e, t)$.

So, by considering the vehicles flow v_q and j_{jam} , it can be modified as [2]

$$E_{\text{con}} = \frac{b_{\text{cap}} \cdot T \cdot v_q}{\text{AER} \cdot j_{\text{jam}}} \quad (49)$$

B. Second Level of ICSA

HGSO has been used to solve the second level of optimization problem. Using the outcome of ILP along with the parameter shown in Section II-E, all the required attributes have been assessed, and the corresponding population sets have been generated. The HGSO is a very recent optimization proposed by Hashim *et al.* [30] and inspired by the nature science-based algorithm.

The stages of HGSO and its corresponding equations have been shown as follows.

Stage 1: The process of Initialization

Within a constraint's boundary or range, a random population can be generated and initialized by

$$Y^i(k+1) = Y_{\min}^k + \text{rand}(Y_{\max}^k - Y_{\min}^k). \quad (50)$$

Stage 2: Clustering and evaluation of Henry's gas constant

$$\begin{cases} H^l(k) = C^1 * \text{rand}(0, 1) \\ p^{i,l} = C^2 * \text{rand}(0, 1) \\ \tilde{C}^{i,l} = C^3 * \text{rand}(0, 1) \end{cases} \quad (51)$$

Stage 3: Updating Henry's coefficient and solubility

$$(H^l(k+1)) = (H^l(k)) \times \exp \left(-\tilde{C}^l \left(\frac{1}{T(k)} - \frac{1}{\tilde{T}} \right) \right) \quad (52)$$

$$\text{sol}^{i,l}(k) = \alpha * H^l(k+1) * p^{i,l}(k). \quad (53)$$

Stage 4: Position update

The positions can be updated using the following equations:

$$\begin{aligned} Y^{i,l}(k+1) &= Y^{i,l}(k) + F * \text{rand} * \sigma * (Y^{\text{best}}(k) - Y^{i,l}(k)) \\ &\quad + F * \text{rand} * \mu \\ &\quad * (\text{sol}^{i,l}(k) * Y^{\text{best}}(k) - Y^{i,l}(k)) \end{aligned} \quad (54)$$

$$\sigma = \beta * \exp(-F^{\text{best}}(k) + \epsilon / F^{i,l}(k) + \epsilon), \quad \epsilon = 0.05. \quad (55)$$

Stage 5: Escape of local optimum and update of the worst agent's position

$$N^{\text{worst}} = N * (\text{rand}(r^2 - r^1) + r^1) \quad (56)$$

$$G^{i,l} = G^{\min(i,l)} + \text{rand}(G^{\max(i,l)} - G^{\min(i,l)}). \quad (57)$$

For further details regarding these above-mentioned equations and nomenclatures, refer [28]. The algorithm of HGSO has been shown in the following part. In Fig. 3, the whole working procedure has been described.

V. PERFORMANCE EVALUATION, RESULTS, AND DISCUSSIONS

A. Test Case-1

This test case has been divided into six subtest cases named TC1a, TC1b, TC1c, TC1d, TC1e, and TC1f with 10, 20, 30, 40, 50, and 60 EVs, respectively, of lower battery capacity (LBC). Each test case consists of three kinds of EVs, such as PHEV-30, PHEV-40, and BEV [29] in the ratio of 70%, 20%, and 10%, whose specifications are given in [27].

B. Test Case-2

In the same manner, test case 2 also has been divided into six subtest cases named TC2a, TC2b, TC2c, TC2d, TC2e, and TC2f with 10, 20, 30, 40, 50, and 60 EVs of higher battery capacity (HBC), and each of them consists of Tesla Roadster [30], BMW Mini E [31], and BEV Version of BMW i3 [31] model EV's in the ratio of 20%, 55%, and 25%, respectively.

C. Input Data

The attributes related to driving cycles, such as t^{arr} , t^{dep} , D , d^f , ETL, and SOC_{ini} are uncertain and to generate these, 2m-PEM has been adopted, as shown in Section III-A, which follows a normal distribution [8], [26]. The data regarding these attributes have been given in Tables III and IV. In Table II, the charging and discharging rates for each charging category have been decided as per the battery capacity of the vehicles, and the charging rates are always greater than the discharging rates [14].

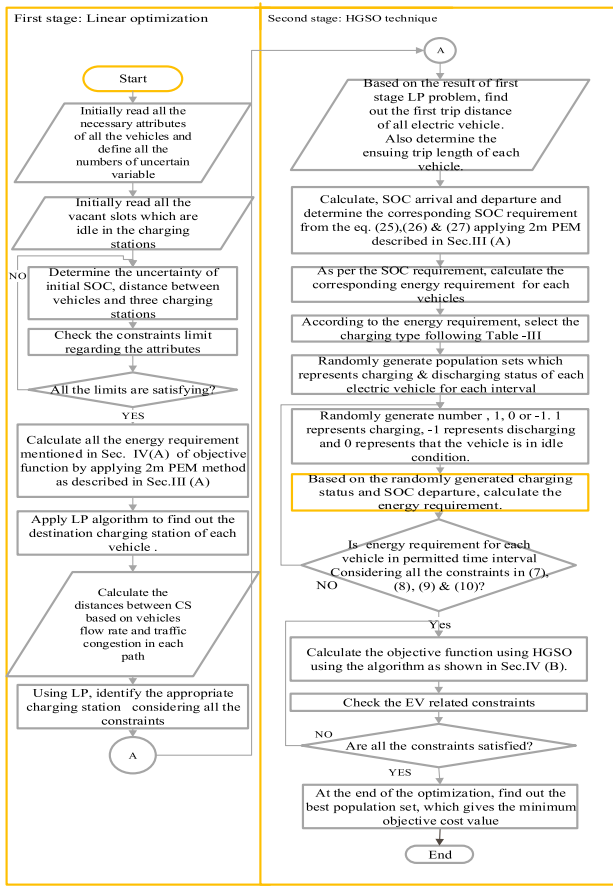


Fig. 3. Basic workflow of ICSA with the HGSO integration.

TABLE II
VARIABLE CHARGING RATES

Ch*. Category	Energy requirement (kWh)	Min. ch ^{rate} /dch ^{rate} (kW)	Max. ch ^{rate} (kW)
Category 1	Energy > 3	-0.005	14
Category 2	0 <= Energy < 3	-0.003	6
Category 3	Energy < 0	-0.8	3

TABLE III
PARAMETERS OF UNCERTAIN ATTRIBUTES

Uncertain Variable	Mean (μ)		St. Deviation (σ)	
	T1	T2	T1	T2
D (km)	55	128	10	10
t ^{arr} (Hrs.)	12	12	2	2.5
t ^{dep} (Hrs.)	16	17	2	2.5

TABLE IV
PARAMETERS OF VEHICLES LOCATION FROM CS

Distance btw. EVs and CS	Mean (μ) (Km.)		St. Deviation (σ) (km.)	
	T1	T2	T1	T2
CS 1	21	60	1.5	1.5
CS 2	20	75	1.73	1.73
CS 3	22	65	1.2	1.2

D. Real-Time Tariff

The information about RTT is highly volatile. The data are taken from NEMS of any particular day [1], where RTT of every half an hour (30 min) interval is provided in Fig. 2.

E. Assumptions

Few assumptions have been considered in ICSA. It is assumed that all these CS are homogeneous regarding the EVSE ratings and each CS have fewer charging points than the total number of vehicles. For example, if total ten EVs are there, then at each CS, five, three, and two charging slots are there, respectively. Likewise, for other test cases also, the number of charging slots at each CS is less than the total number of vehicles. CSs are situated near the public areas, such as schools, markets, and universities, where EVs can stay for at least a couple of hours. In Table II, three types of charging categories have been set, as per the energy demand by the EVs and accordingly, two input data, i.e., min. charging rate (or discharging rate) and max. charging rate are there for each type of charging category [14], [15].

F. Results and Discussions

As per the problem formulation, in the first level of ICSA, appropriate CS has been allotted to each PEV with the minimum energy consumption of the battery. Thereafter, considering all the constraints, as mentioned in (42)–(44) and as per the FTD and ETL, the values of SOC^{arr} [see Fig. 5(a1) and (a2)] and SOC^{dep} [see Fig. 5(b1) and (b2)], the SOC^{req} [see Fig. 5(c1) and (c2)] and its corresponding eng^{req} [see Fig. 5(d1) and (d2)] has been determined for TC1a and TC2a, where ten EVs of LBC and HBC are considered. Likewise, for other test cases also, a similar kind of operation has been performed.

Using these calculated attributes, in the second level of the ICSA, the HGSO optimization has been applied to evaluate the objective function, i.e., total daily price incurred by CSO and its corresponding charging strategies, as shown in Fig. 6, where black blocks are representing the V2G mode of operations and white blocks are representing the G2V mode of operations, and the rest of the Grey blocks are idle. From TC1a–TC1f, it can be observed that, due to the majority of LBC EVs, most of the time, each and every EV is participating more in the G2V mode of operations and for very few times it is changing its switching sequence from the G2V mode to the V2G mode of operations. But as EVs are increasing from 10 to 60, it can also be noticed that gradually the V2G mode of operations is increasing, but then also in several cases, despite higher RTT, EVs are participating in the G2V mode, rather than the V2G mode of operation.

Unlike the former scenario, if the charging strategies of TC2a–TC2f are observed, then it can be realized that, due to the majority of HBC EVs, when the RTT is higher, EVs are participating in the V2G mode of operation and when RTT is lower, it is participating in the G2V mode of operations, which is actually required for the minimization of the daily price incurred by CSO. When the number of EVs is increasing, it can be seen that the V2G mode

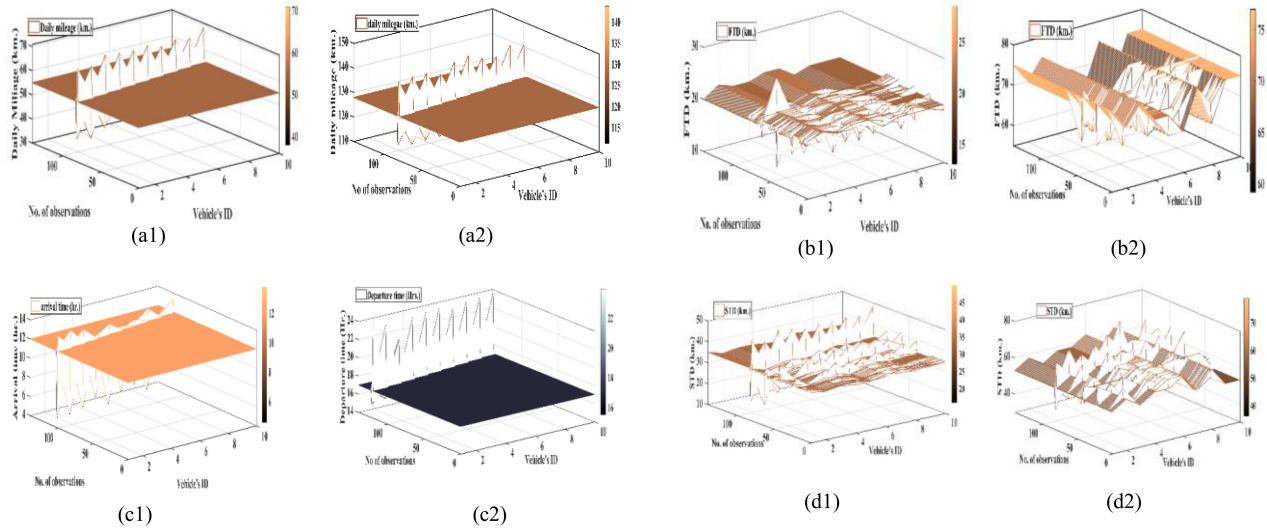


Fig. 4. For TC1a and TC2a. (a1) and (a2) Estimated daily mileage of ten LCB and ten HCB. (b1) and (b2) Estimated first trip distance of ten LCV and ten HCB. (c1) and (c2) Estimated arrival time and departure time of both ten LCB and HCB. (d1) and (d2) Ensuing trip length of ten LCB and ten HCB.

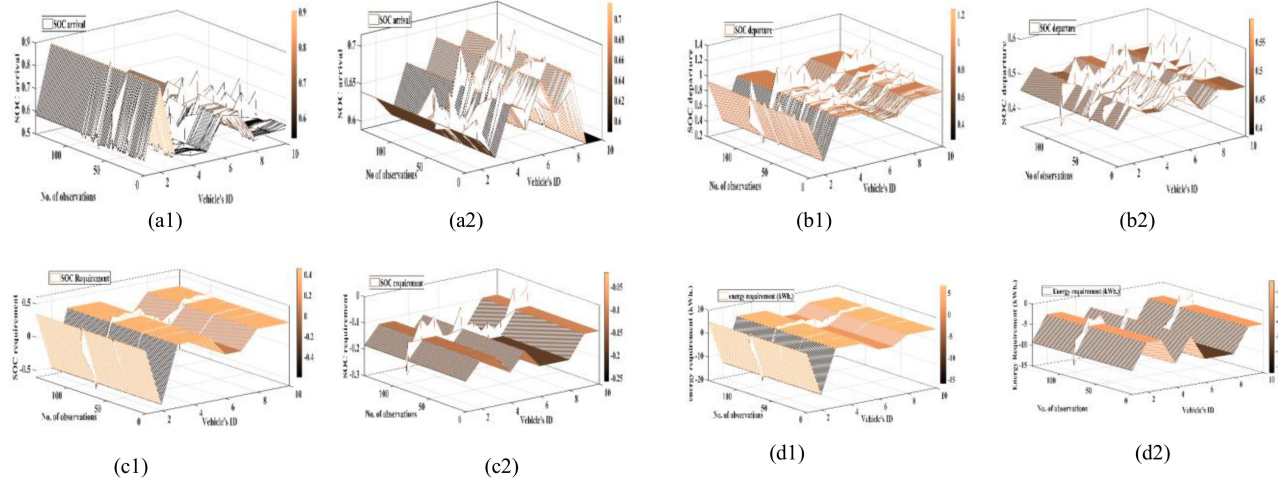


Fig. 5. For TC1a and TC2b. (a1) and (a2) Calculated SOC^{arr} of ten LCB and ten HCB. (b1) and (b2) Calculated SOC^{dep} of ten LCV and ten HCB. (c1) and (c2) Calculated SOC^{req} of both ten LCB and ten HCB. (d1) and (d2) Calculated eng^{req} of ten LCB and ten HCB of operation can be possible.

of operations is increasing than the G2V mode of operations for each and every EV. Therefore, comparing these two scenarios, it can be said that, if the number of EVs is more having HBC, then better coordination between the G2V mode of operation and V2G mode of operation can be possible.

Nevertheless, irrespective of LBC EVs or HBC EVs, the coordination of this dual mode of operation is always beneficial for both CSO and EV owner.

In support of this claim, a critical analysis has been performed by taking a subtest case TC1a, where ten LBC EVs are there, and among them, the fifth number EV has been taken to demonstrate the benefit. From Fig. 6(a1), it can be noticed that the fifth EV enters the CS at slot 22 and the departure slot is 43. Now, as per the vehicle's daily mileage [see Fig. 4(a1)], FTD [see Fig. 4(b1)], ETL [see Fig. 4(d1)], and that very vehicle's AER, SOC arrival,

SOC departure, SOC requirement, and its corresponding energy requirement have been calculated, which are 58.884%, 82.018%, and 4.48047 kWh, respectively. This needs to be kept in mind that the departure slot has been chosen by the EV user only. Within this interval, the CSO needs to meet the energy demand of that EV. Consequently, optimization has been performed using (11), to keep the total daily price incurred by CSO at optimum. The charging strategy of the fifth EV has been shown in the first row of Fig. 9, where both G2V and V2G modes of operation have been performed. On the other hand, in the second row, the charging strategy using only the G2V mode of operation has been shown. As per the RTT, if the cost of these two operations can be compared, then from Table V, it can be realized that the combination of both G2V and V2G modes of operation is always beneficial for CSO, as it is getting a profit of 0.205385

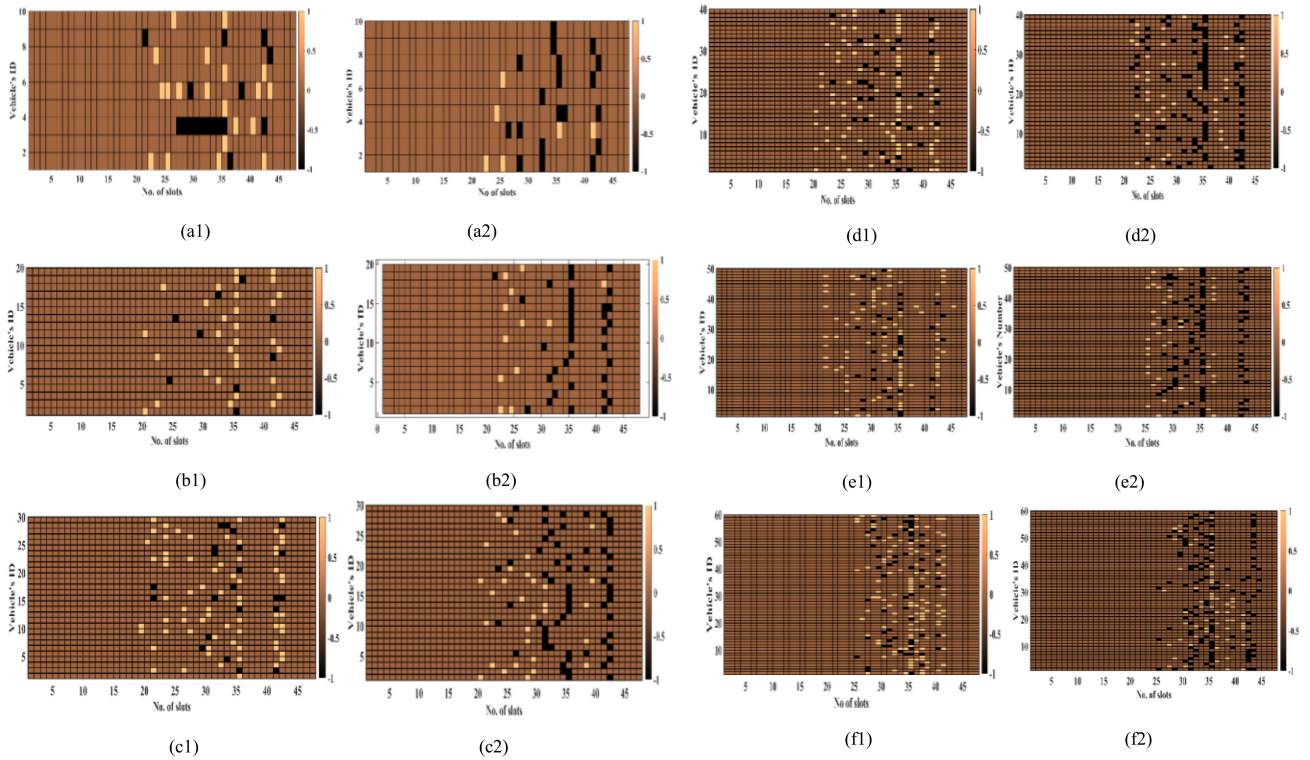


Fig. 6. For test cases 1 and 2: (a1) and (a2) charging strategy of TC1a and TC2a; (b1) and (b2) charging strategy of TC1b and TC2b; (c1) and (c2) charging strategy of TC1c and TC2c; (d1) and (d2) charging strategy of TC1d and TC2d; (e1) and (e2) charging strategy of TC1e and TC2e; (f1) and (f2) charging strategy of TC1f and TC2f.

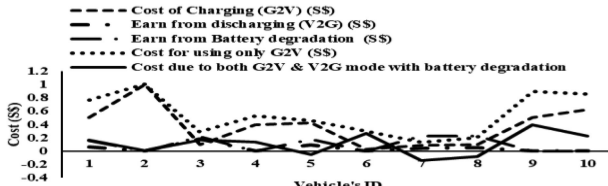


Fig. 7. Cost comparison of TC1a.

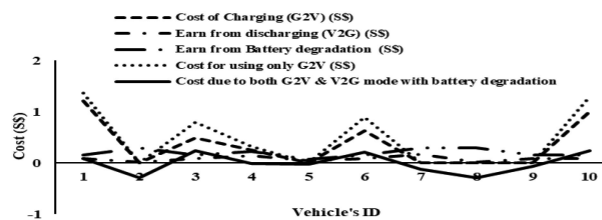


Fig. 8. Cost comparison of TC2a.

\$. Moreover, after comparing the costing between only the G2V mode of operation and dual mode of operation of TC1a and TC2a, from Figs. 7 and 8, it can be observed that, for every individual case, the CSO is getting more profit by conducting the dual mode of operation rather performing only the G2V mode of operation and in case of HBC EVs, the margin of profit is more.

Again, for TC1e and TC2e, having 50 LBC EVs and 50 HBC EVs, a similar kind of analysis has been performed. Between

TABLE V
VARIOUS COST OF THE FIFTH EV IN TC1a

$Cost^{och}$ (\$S\$)	$Cost_{batt.deg}$ (\$S\$)	Cost for using only G2V (\$S\$)	Profit (\$S\$)
0.423402	0.1761	0.45268	0.205385

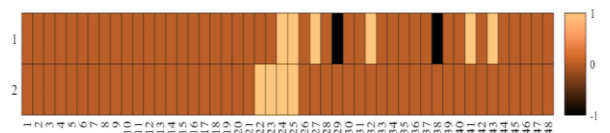


Fig. 9. Charging strategy for the fifth EV of TC1a.

these two test cases, from Figs. 10 and 12, it can be analyzed that, due to more LBC EVs, the margin of profit for the dual mode of operation is less. On the other hand, for TC2e, if Figs. 11 and 13 can be realized, then it can be said that, due to the presence of more HBC EVs, more amount of V2G operations is occurring. Therefore, the margin of profit for CSO is also getting higher. Although for both the scenarios, CSO is gaining profit as it is earning more from the grid by performing more V2G mode of operation. After performing the coordinate charging, it can be observed from Fig. 14 that, for both test cases with the increase of set of EVs from 10 to 60, the cost of charging is increasing. But, in comparison with HBC EVs in test case 2's scenarios, the cost of the G2V mode of operation is more for LBC EVs under test case 1. Again, if only the cost of V2G mode can be

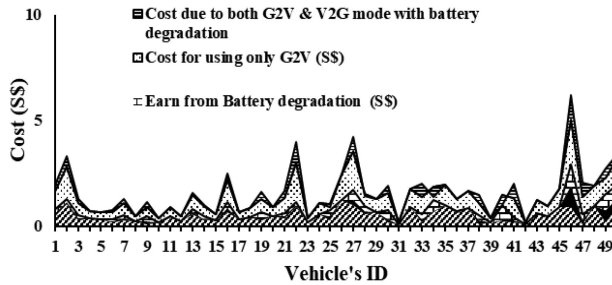


Fig. 10. Comparison of individual costs of TC1e.

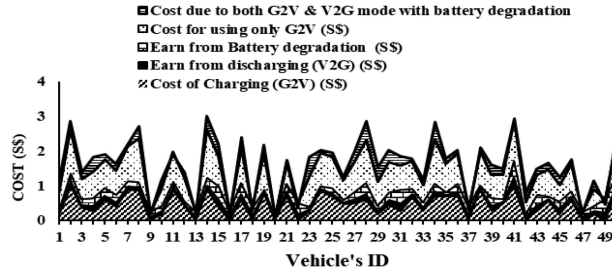


Fig. 11. Comparison of individual costs of TC2e.

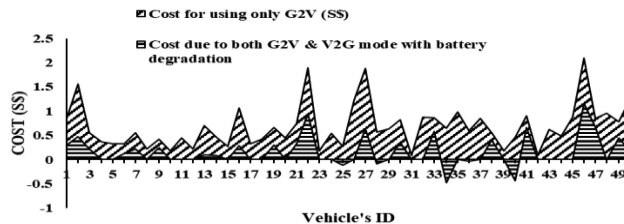


Fig. 12. Overall cost comparison between only the G2V mode and combination of both G2V and V2G modes for TC1e.

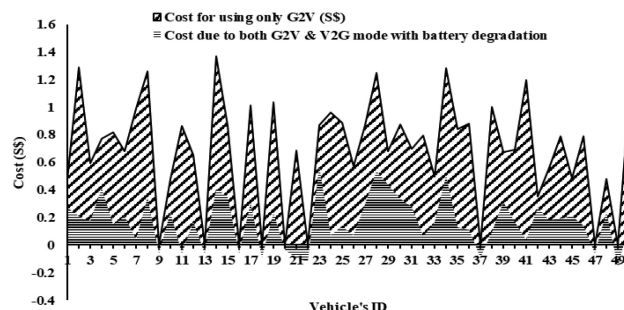


Fig. 13. Overall cost comparison between only the G2V mode and combination of both G2V and V2G modes for TC2e.

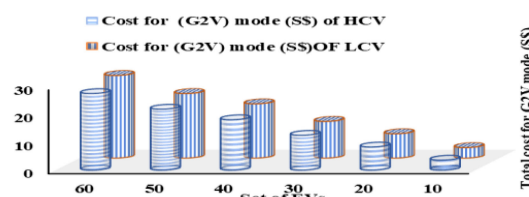


Fig. 14. Comparison of cost for the G2V mode of operation between LBC and HBC EV.

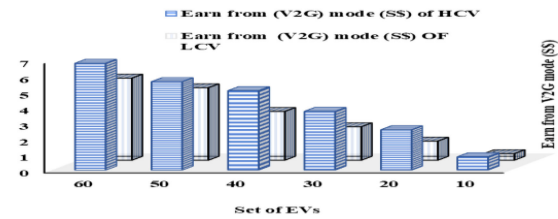


Fig. 15. Comparison of earning from the V2G mode of operation between LBC and HBC EV.

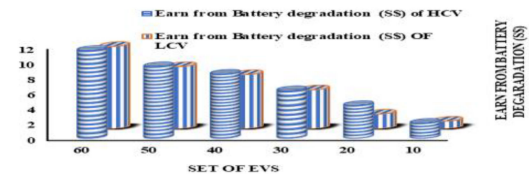


Fig. 16. Comparison of earning from the battery degradation for the V2G mode of operation between LBC and HBC EV.

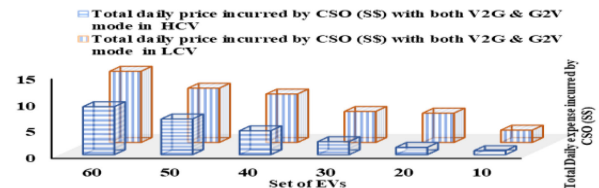


Fig. 17. Comparison of the total daily price incurred by CSO for both G2V and V2G modes of operation between LBC and HBC EV.

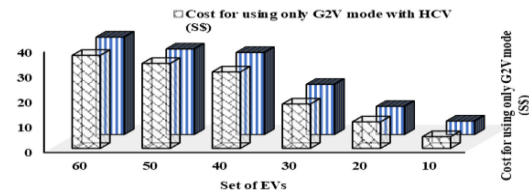


Fig. 18. Comparison of cost for only the G2V mode of operation between LBC and HBC EV.

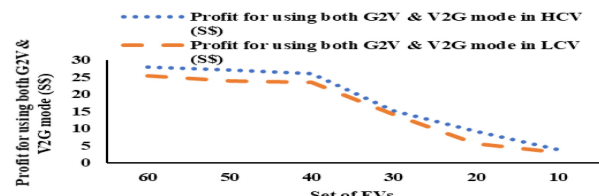


Fig. 19. Comparison of profit incurred by CSO for both G2V and V2G modes of operation between LBC and HBC EV.

considered, then from Fig. 15, it can be observed that the earning of revenue from the V2G mode is increasing with the increment of EVs for both the test cases. But, compared with LBC EVs, the earning of revenue is more for HBC EVs. Since the earning of revenue from battery degradation is correlated with the V2G mode of operation, thus, from Fig. 16 also, the same kind of scenario can be observed. On the contrary, when only the G2V mode of operation has been considered, for all the test systems, then it can be assessed that, with the increase of EVs, the cost

TABLE VI
COMPARISON OF TOTAL COSTS AND PROFITS CONSIDERING BOTH G2V AND V2G MODES OF OPERATION FOR ALL THE TEST CASES UNDER TEST CASES 1 AND 2

SET OF VEHICLES	CC=Cost of Charging (G2V) (\$\$)	ED=Earn from discharging (V2G) (\$\$)	OC=Overall cost (G2V+V2G) (\$\$)	EBD=Earn from Battery degradation (\$\$)	DTP=CC-ED-EBD (\$\$)	COC=Cost for only G2V (\$\$)	PROFIT=COC-DTP (\$\$)
60 HCV	27.406197	6.835975	20.570222	11.432545	9.0924222	37.0921142	27.999692
60 LCV	29.5531	5.2549	24.2982	10.82998	13.46822	38.8931	25.42488
50 HCV	21.8175411	5.659225	16.158316	9.3983329	6.7599832	33.8984975	27.138514
50 LCV	23.085299	4.64203	18.443269	8.1710649	10.272204	34.1424912	23.870287
40 HCV	18.0352341	5.08368	12.951554	8.4211334	4.5304207	30.4931116	25.962691
40 LCV	19.408728	3.12364	16.285088	7.1250335	9.1600545	32.7412559	23.581201
30HCV	12.475328	3.7577	8.717628	6.2426725	2.4749555	17.6941954	15.21924
30 LCV	13.12811	2.141523465	10.986587	5.1131969	5.8733896	20.0334047	14.160015
20HCV	8.2795962	2.580725	5.6988712	4.2863015	1.4125697	10.5870207	9.174451
20LCV	8.70302	1.222465	7.480555	1.9257754	5.5547796	11.2453444	5.6905648
10HCV	3.579008	0.847096	2.731912	1.9548548	0.7770572	4.66771385	3.8906566
10LCV	3.73853	0.41564	3.32289	0.9945182	2.3283718	5.39730185	3.0689301

TABLE VII
COMPARISON OF COSTS BY APPLYING ICSA WITH 2m-PEM AND MCS TECHNIQUE BY CLUBBING VARIOUS OPTIMIZATION

ICSA with 2m PEM method FOR TC2a (10 EV of HBC)								
	HGSO	GWO	BBO	BA	SOS	DE	GA	PSO
Min Cost (\$\$)	0.777057	0.98305	1.01223	1.8703	2.0139	2.591	2.9918	3.2109
Avg. Cost (μ)	1.011617333	1.202166547	1.63668120	2.32431625	2.49154184	2.89384861	3.40608446	3.54285998
Standard dev (σ)	0.127423065	0.156789463	0.45467328	0.27967470	0.27042156	0.1862756	0.20925021	0.20154547
ICSA with MCS method FOR TC2a (10 EV of HBC)								
Min Cost (\$\$)	1.5929585	1.9902369	2.213368	2.855699	3.5223647	3.995223	4.2235852	4.89933
Avg. Cost (μ)	2.18838725	2.60858895	20055112.6	4.151316	5.26181135	5.7532838	6.1129201	6.634576
Standard dev (σ)	0.620096423	0.7200369	0.6510025	0.885691	0.5533301	0.6552558	0.8899202	0.5220336
ICSA with 2m PEM method FOR TC1a (10 EV of LBC)								
Min Cost (\$\$)	2.328372	2.89125	3.02512	3.8123	4.11029	4.51981	4.98101	5.09812
Avg. Cost (μ)	2.763815343	3.222906126	3.49404898	4.05007698	4.60468702	4.89073154	5.51321172	5.58601631
Standard dev (σ)	0.287095826	0.16417202	0.21790063	0.1388538	0.30104026	0.20306381	0.31279662	0.31595540
ICSA with MCS method FOR TC1a (10 EV of LBC)								
Min Cost (\$\$)	3.891123	4.0012369	4.559315	5.001369	5.886931	6.223001	6.4558226	7.00012258
Avg. Cost (μ)	4.7802265	5.11246345	5.7747682	6.44550665	6.9453125	8.123185	8.50739445	9.01124889
Standard dev (σ)	0.559331	0.612234	0.5568	0.75513	0.7880445	0.801125	0.744696	0.533696
ICSA with 2m PEM method FOR TC2b (20 EV of HBC)								
Min Cost (\$\$)	1.4134	1.8973	2.1915	2.8135	3.108	3.4632	3.7563	4.458
Avg. Cost (μ)	1.713865486	2.183949691	2.77270746	2.99682063	3.47591367	3.73081674	4.08809741	4.89282308
Standard dev (σ)	0.206060581	0.196012769	0.34475741	0.12401925	0.26364924	0.16888405	0.24016332	0.23827899
ICSA with MCS method FOR TC2b (20 EV of HBC)								
Min Cost (\$\$)	2.51447	3.9982236	4.225336	4.558963	5.002235	5.5663147	6.001125	6.455863
Avg. Cost (μ)	3.70393	4.5004033	5.1137955	5.7626605	6.114049	6.76630995	7.011847	7.5073425
Standard dev (σ)	0.7442588	0.523658	0.589932	0.889228	0.711459	0.66311478	0.5569248	0.66821445
ICSA with 2m PEM method FOR TC1b (20 EV of LBC)								
Min Cost (\$\$)	5.55478	5.9899	6.21985	6.82158	7.00215	7.51289	8.01285	8.43551
Avg. Cost (μ)	5.906024563	6.389114156	6.65886561	7.12132050	7.53685590	7.88455941	8.37396977	8.69797794
Standard dev (σ)	0.289584132	0.303308517	0.37212055	0.44052194	0.36263487	0.38673666	0.31956906	0.41197838
ICSA with MCS method FOR TC1b (20 EV of LBC)								
Min Cost (\$\$)	6.889335	7.22350115	7.995255	8.6698522	9.223688	9.889932	10.0228484	10.57663
Avg. Cost (μ)	7.4459615	7.895217075	8.508919	9.46440775	10.056659	10.5743975	10.9611057	11.41624
Standard dev (σ)	0.5699931	0.4589933	0.7882361	0.6688952	0.5589633	0.68723131	0.589996	0.6998412
ICSA with 2m PEM method FOR TC2c (30 EV of HBC)								
Min Cost (\$\$)	2.474	2.9152	3.21229	3.81805	4.00123	4.51981	4.89512	5.02897
Avg. Cost (μ)	2.811113678	3.171969726	3.78263954	4.17473589	4.48157864	4.87162133	5.38301589	5.43280364
Standard dev (σ)	0.261107497	0.151182421	0.30258006	0.16243651	0.29358421	0.20093200	0.25910448	0.30285889
ICSA with MCS method FOR TC2c (30 EV of HBC)								
Min Cost (\$\$)	3.589633	3.985536	4.225886	4.8963314	5.558833	6.22598742	6.9002858	7.228863
Avg. Cost (μ)	4.589783	5.004058	5.2923445	5.9494447	6.7242335	7.22593521	7.87799105	8.2264145
Standard dev (σ)	0.5229722	0.7822363	0.8993333	0.812588	0.669822	1.022288	0.58901115	0.6998522

of charging is increasing, and there is no question of earning revenues.

Hence, after combining the above-mentioned three scenarios, it can be said that, if the combination of G2V and V2G mode of operation can be performed instead of only the G2V mode of

operation, then for all the test cases, both CSO and EV owner will gain profit and with the increment in the number of EVs, this profit will arise more. At the same time, the margin of profit will be more for HBC EVs, as shown in Fig. 19. The overall comparison of total costs and profits, with the increment of EVs

TABLE VII
CONTINUED

	ICSA with 2m PEM method FOR TC1c (30 EV of LBC)							
Min Cost (\$\$)	5.87339	6.00179	6.51389	7.00258	7.81239	8.21597	8.5902	9.00125
Avg. Cost (μ)	6.33402701	6.466110456	7.08644420	7.61692156	8.20520292	8.70464786	9.03768473	9.56153631
Standard dev (σ)	0.321453529	0.247935425	0.29966502	0.40226908	0.31555966	0.31624786	0.24729921	0.31285857
	ICSA with MCS method FOR TC1c (30 EV of LBC)							
Min Cost (\$\$)	6.922447	7.258899	7.9665852	8.53394556	8.98822366	9.15993258	9.893366	10.225886
Avg. Cost (μ)	7.5782185	8.105619	8.4895212	9.21178953	9.67910483	10.0299312	10.447977	11.0627595
Standard dev (σ)	0.8993314	0.65889634	0.55772413	0.6997422	0.5589993	0.6988563	0.788922	0.66985223
	ICSA with 2m PEM method FOR TC2d (40 EV of HBC)							
Min Cost (\$\$)	4.5312	4.99512	5.4381	5.8128	6.02187	6.81229	7.00125	7.8122
Avg. Cost (μ)	4.740752612	5.163554157	6.08386342	6.07319814	6.68505311	7.21433055	7.60202342	8.16559240
Standard dev (σ)	0.289584132	0.303308517	0.37212055	0.44052194	0.36263487	0.38673666	0.31956906	0.41197838
	ICSA with MCS method FOR TC2d (40 EV of HBC)							
Min Cost (\$\$)	5.9885285	6.878989	7.022583	7.7882263	8.002588	8.5669901	9.118884	9.788926
Avg. Cost (μ)	6.94423075	7.5124345	7.9596185	8.40540715	8.9509101	9.31144005	9.887388	10.395607
Standard dev (σ)	0.568998	0.6684102	0.78212656	0.6698452	0.500258	0.5699924	0.665889	0.88952994
	ICSA with 2m PEM method FOR TC1d (40 EV of LBC)							
Min Cost (\$\$)	9.160055	9.81287	10.02983	10.5283	11.00259	11.689679	11.9981	12.21289
Avg. Cost (μ)	9.589343515	10.34806527	10.9633595	11.2708591	11.7214783	12.3883219	12.6174962	12.8910488
Standard dev (σ)	0.310189944	0.333775883	0.46977416	0.46662117	0.39283771	0.33966173	0.36324172	0.47054614
	ICSA with MCS method FOR TC1d (40 EV of LBC)							
Min Cost (\$\$)	10.69986	11.022886	11.89933	12.66994	13.02258	13.899302	14.098323	14.829201
Avg. Cost (μ)	11.34919	12.022888	12.729645	13.347915	14.32927	14.955367	15.440178	16.0995755
Standard dev (σ)	0.5699826	0.698852	0.5660058	0.6888216	0.699822	0.78925	0.687822	0.8992851
	ICSA with 2m PEM method FOR TC2e (50 EV of HBC)							
Min Cost (\$\$)	6.7592	6.89828	7.02458	7.5948	7.98345	8.1985	8.76321	9.00156
Avg. Cost (μ)	7.291293109	7.448725297	7.55571985	7.90445804	8.50750058	8.72237385	9.25019521	9.94818676
Standard dev (σ)	0.308109932	0.284576159	0.32668635	0.18795273	0.28448273	0.31575532	0.31610756	0.61526245
	ICSA with MCS method FOR TC2e (50 EV of HBC)							
Min Cost (\$\$)	7.899613	8.237966	8.9833369	9.301479	9.878933	10.325599	10.9886	11.58933
Avg. Cost (μ)	8.4612355	9.24697	9.88665095	10.2292345	10.9384735	11.5839295	12.05224	12.6097375
Standard dev (σ)	0.503699	0.689946	0.7896223	0.5588233	0.789933	0.987269	0.658816	0.5999234
	ICSA with 2m PEM method FOR TC1e (50 EV of LBC)							
Min Cost (\$\$)	10.2835	10.98105	11.358105	11.89088	12.12589	12.88125	13.00129	13.49812
Avg. Cost (μ)	10.77109704	11.49389027	11.8760138	12.5503552	12.8887228	13.5105982	13.6274324	14.0048664
Standard dev (σ)	0.378252088	0.265606142	0.34490566	0.38431715	0.45389885	0.32539477	0.36246912	0.31848516
	ICSA with MCS method FOR TC1e (50 EV of LBC)							
Min Cost (\$\$)	11.6998781	12.03699	12.899632	13.25588	14.002588	14.58964	15.025993	15.85666
Avg. Cost (μ)	12.29960405	13.368356	14.079261	14.529785	15.300974	15.79611	16.507428	17.061825
Standard dev (σ)	0.5993344	0.652369	0.5993113	0.6488933	0.782226	0.7922456	0.605879	0.599633
	ICSA with 2m PEM method FOR TC2f (60 EV of HBC)							
Min Cost (\$\$)	9.0924	10.0145	10.8945	11.4245	11.8891	12.0021	12.8123	13.0123
Avg. Cost (μ)	9.624632225	10.54830839	11.3827001	12.2157566	12.4754339	12.5060311	13.3027713	13.7994689
Standard dev (σ)	0.289584132	0.303308517	0.37212055	0.44052194	0.36263487	0.38673666	0.31956906	0.41197838
	ICSA with MCS method FOR TC2f (60 EV of HBC)							
Min Cost (\$\$)	10.899012	11.899332	12.36841	13.02588	13.923478	14.6987463	15.0036478	15.8543641
Avg. Cost (μ)	11.4395795	12.943377	13.469155	14.024234	14.9054705	15.4661166	16.0995389	16.9199636
Standard dev (σ)	0.5963245	0.658942	0.784469	0.8782233	0.698523	0.596641	0.6574692	0.7566933
	ICSA with 2m PEM method FOR TC1f (60 EV of LBC)							
Min Cost (\$\$)	13.46822	13.89826	14.01223	14.5189	14.9124	15.0211	15.8951	16.0122
Avg. Cost (μ)	13.71659565	14.47258802	14.4441644	15.0346566	15.3693214	15.6351270	16.2660380	16.5312872
Standard dev (σ)	0.167120044	0.310960017	0.26410168	0.33235005	0.31473048	0.36945240	0.22347598	0.33534990
	ICSA with MCS method FOR TC1f (60 EV of LBC)							
Min Cost (\$\$)	14.89932	15.2558	15.890123	16.20258	17.66993	18.09215	18.899012	19.02258
Avg. Cost (μ)	15.463888	16.06663	16.461635	17.2858511	18.5957	19.3634705	19.951463	20.346245
Standard dev (σ)	0.5966471	0.66780336	0.781223	0.899663	0.9788012	0.6933146	0.7989336	0.8469935

DE: Differential evolution; BBO: Biogeography-based optimization; GWO: Grey-wolf optimization; SOS: Sum of square optimization; BA: Bat algorithm; PSO: Particle swarm optimization; GA: Genetic algorithm.

for both the test cases have been shown in Table VI. Hence, from Table VI and Figs. 14–19, it can be observed that, with the increase of LBC EVs, the profit will increase. But, compared with the EVs having HBC, the margin of profit is lower.

Now, in order to establish the robustness of the ICSA, various optimization techniques, such as differential evolution, biogeography-based optimization, grey-wolf optimization, sum

of square optimization, bat algorithm, particle swarm optimization, and genetic algorithm, have been applied to verify its performance. From Table VII, by observing the mean and standard deviation of the costs, it can be said that ICSA is robust enough to give consistent outputs for all the test cases by clubbing HGSO. Moreover, to analyze the performance of 2m-PEM, it has been compared with the MCS method [18] after 50 trial runs, and from

TABLE VIII
WSRT RESULT FOR TEST CASES 1 AND 2

Optimization	Test statistic value					
	TC1a	TC1b	TC1c	TC1d	TC1 e	TC1f
HGSO	193	196.5	227.5	217.0	202.0	221.5
GWO	171	228.5	194.5	162.0	217.0	188.5
BBO	214.5	229.0	186	208.0	231.0	206.5
BA	226	175.0	224	175.0	194.5	192.0
SOS	193.5	203.0	153	169.0	210.0	230.5
DE	218	224.5	202	205.0	192.0	210.0
GA	217	224.5	176	209.0	230.5	212.0
PSO	216.5	207.0	209.5	171.0	188	209.5
	TC2a	TC2b	TC2c	TC2d	TC2 e	TC2f
HGSO	182	218.5	189	185.0	229.5	202.0
GWO	196.5	201.0	208.5	151.5	229.0	202.5
BBO	196.5	216.0	219.0	200.5	205	215.0
BA	225	176.0	194.5	228.0	170	216.5
SOS	191	210.5	204.0	201.5	202.0	217.5
DE	227	219.5	202.5	171.5	213.0	195.5
GA	213	201.0	226.0	227.5	214.0	218.0
PSO	182.5	215.0	185.5	192.5	214.0	214.5

TABLE IX
QT RESULT FOR TEST CASES 1 AND 2

No of samples	Test statistic value					
	TC1a	TC1b	TC1c	TC1d	TC1 e	TC1f
30	79.17	80.61	74.06	64.19	80.51	69.90
	TC2a	TC2b	TC2c	TC2d	TC2 e	TC2f
30	71.69	86.10	72.69	72.17	78.46	69.86

Table VII, by observing the best value and standard deviation, it can be said that, 2m-PEM is superior in comparison with the MCS method. Moreover, the time of simulation is much higher for the MCS method, compared with the 2m-PEM. This is how the superiority of the 2m-PEM for handling the uncertainty in the proposed ICSA algorithm can be established.

1) *WSRT and Quade Test:* For both test case 1 (TC1a–TC1f) and 2 (TC2a–TC2f), WSRT [34] and QT [34] have been performed (at a 95% confidence interval) by simulating each test case for 30×. The absolute value for 30 samples is 137 (from α -distribution table). From Table VIII, it is hereby observed that for every test case the test statistic value is higher than the absolute value. This implies the acceptance of null hypothesis H_0 , which further shows the consistency and sturdiness of optimization techniques in ICSA. Likewise, in the QT, from Table IX, it can be observed that for both T_1 and T_2 , the test statistic value is greater than its absolute value (i.e., 2.04 for 30 samples) as obtained from the f -distribution table. This infers rejection of null hypothesis H_0 , i.e., applying HGSO results in a significant change as compared with another optimization techniques in ICSA.

VI. CONCLUSION

In this article, by applying the proposed ICSA, EVs have been allocated at appropriate CS. Thereafter, the minimization of the total daily price acquired by CSO is determined and its conforming charging scheduling has been set on. As per the energy requirement, the charging scheduling is done by keeping the vehicles in the G2V, V2G, and idle mode. The significance of coordination of the G2V mode and V2G mode of operation has been analyzed and it has been showed that both CSO and EV owner can be in a beneficial position. Moreover, it has been detected that, with the increase of EVs along with its battery

capacity, the margin of profit from charging scheduling will be greater. Likewise, for better coordination of the G2V and V2G mode of operation, a greater number of vehicles with HBC are desirable. Thereafter, from the results it has been observed that 2m-PEM is superior regarding the handling of uncertain variables. Furthermore, the results after applying HGSO have been compared with the other optimization techniques and it has been observed that HGSO is superior to others. Later, by the statistical analysis, it can be said that the proposed ICSA in coordination with the optimization techniques is robust enough to produce consistent output for both lower and higher number of vehicles.

REFERENCES

- [1] S. Das, P. Acharjee, and A. Bhattacharya, "Charging scheduling of electric vehicle incorporating grid-to-vehicle (G2V) and vehicle-to-grid (V2G) technology in smart-grid," in *Proc. IEEE Int. Conf. Power Electron., Smart Grid Renewable Energy*, Kerala, India, Jan. 2–4, 2020, pp. 1–6.
- [2] R. Mkahl, "Contribution to the modeling, dimensioning and management of the energy flows of an electric vehicle charging system: Study of the interconnection with the electric network," Ph.D. dissertation, Dept. Eng. Sci. Microengineering, Univ. Technol. Belfort-Montbéliard, Belfort, France, 2015.
- [3] D. Wu, D. C. Aliprantis, and L. Ying, "Load scheduling and dispatch for aggregators of plug-in electric vehicles," *IEEE Trans. Smart Grid*, vol. 3, no. 1, pp. 368–376, Mar. 2012.
- [4] F. Zhang, X. Hu, R. Langari, and D. Cao, "Energy management strategies of connected HEVs and PHEVs: Recent progress and outlook," *Prog. Energy Combustion Sci.*, vol. 73, pp. 235–256, Jul. 1, 2019.
- [5] X. Liu and Z. Bie, "Optimal allocation planning for public EV charging station considering AC and DC integrated chargers," *Energy Procedia*, vol. 159, pp. 382–387, Feb. 2019.
- [6] K. Saichand and V. John, "A time-varying virtual resistance control for ultracapacitor based dc–dc converters," *IEEE Trans. Veh. Technol.*, vol. 68, no. 6, pp. 5548–5556, Apr. 2019.
- [7] C. Ma, J. Rautiainen, D. Dahlhaus, A. Lakshman, J.-C. Toebermann, and M. Braun, "Online optimal charging strategy for electric vehicles," *Energy Procedia*, vol. 73, pp. 173–181, Jun. 2015.
- [8] A. Ehsan and Q. Yang, "Active distribution system reinforcement planning with EV charging stations—Part I: Uncertainty modeling and problem formulation," *IEEE Trans. Sustain. Energy*, vol. 11, no. 2, pp. 970–978, Apr. 2020.
- [9] A. Abdalrahman and W. Zhuang, "PEV charging infrastructure siting based on spatial-temporal traffic flow distribution," *IEEE Trans. Smart Grid*, vol. 10, no. 6, pp. 6115–6125, Nov. 2019.
- [10] Y. Ota, H. Taniguchi, T. Nakajima, K. M. Liyanage, J. Baba, and A. Yokoyama, "Autonomous distributed V2G (vehicle-to-grid) satisfying scheduled charging," *IEEE Trans. Smart Grid*, vol. 3, no. 1, pp. 559–564, Mar. 2012.
- [11] E. Sortomme, M. M. Hindi, S. D. J. MacPherson, and S. S. Venkata, "Coordinated charging of plug-in hybrid electric vehicles to minimize distribution system losses," *IEEE Trans. Smart Grid*, vol. 2, no. 1, pp. 198–205, Mar. 2011.
- [12] R. Zgheib, K. Al-Haddad, and I. Kamwa, "V2G, G2V and active filter operation of a bidirectional battery charger for electric vehicles," in *Proc. IEEE Int. Conf. Ind. Technol.*, Taipei, Taiwan, 2016, pp. 1260–1265.
- [13] M. C. B. P. Rodrigues, I. D. N. Souza, A. A. Ferreira, P. G. Barbosa, and H. A. C. Braga, "Simultaneous active power filter and G2V (or V2G) operation of EV on-board power electronics," in *Proc. 39th Annu. Conf. IEEE Ind. Elect. Soc.*, Vienna, Austria, 2013, pp. 4684–4689.
- [14] A. Mohamed, V. Salehi, T. Ma, and O. Mohammed, "Real-time energy management algorithm for plug-in hybrid electric vehicle charging parks involving sustainable energy," *IEEE Trans. Sustain. Energy*, vol. 5, no. 2, pp. 577–586, Apr. 2014.
- [15] L. Gan, U. Topcu, and S. H. Low, "Stochastic distributed protocol for electric vehicle charging with discrete charging rate," in *Proc. IEEE Power Energy Soc. Gen. Meeting*, San Diego, CA, USA, 2012, pp. 1–8.

- [16] J. Rios-Torres, J. Liu, and A. Khattak, "Fuel consumption for various driving styles in conventional and hybrid electric vehicles: Integrating driving cycle predictions with fuel consumption optimization," *Int. J. Sustain. Transp.*, vol. 13, no. 2, pp. 123–137, Feb. 2019.
- [17] P. Ping, W. Qin, Y. Xu, C. Miyajima, and K. Takeda, "Impact of driver behavior on fuel consumption: Classification, evaluation and prediction using machine learning," *IEEE Access*, vol. 7, pp. 78515–78532, 2019.
- [18] D.-M. Kim, P. Benoliel, D.-K. Kim, T. H. Lee, J. W. Park, and J.-P. Hong, "Framework development of series hybrid powertrain design for heavy-duty vehicle considering driving conditions," *IEEE Trans. Veh. Technol.*, vol. 68, no. 7, pp. 6468–6480, Jul. 2019.
- [19] C. Barrows *et al.*, "The IEEE reliability test system: A proposed 2019 update," *IEEE Trans. Power Syst.*, vol. 35, no. 1, pp. 119–127, Jan. 2020.
- [20] Z. Qin *et al.*, "A universal approximation method and optimized hardware architectures for arithmetic functions based on stochastic computing," *IEEE Access*, vol. 8, pp. 46229–46241, 2020.
- [21] C. Li, Y. Chen, T. Ding, Z. Du, and F. Li, "A sparse and low-order implementation for discretization-based eigen-analysis of power systems with time-delays," *IEEE Trans. Power Syst.*, vol. 34, no. 6, pp. 5091–5094, Nov. 2019.
- [22] A. Saha, A. Bhattacharya, P. Das, and A. K. Chakraborty, "A novel approach towards uncertainty modeling in multiobjective optimal power flow with renewable integration," *Int. Trans. Elect. Energy Syst.*, vol. 29, no. 12, Dec. 2019, Art. no. e12136.
- [23] W. Kempton and J. Tomic, "Vehicle-to-grid power fundamentals: Calculating capacity and net revenue," *J. Power Sources*, vol. 144, pp. 268–279, Jun. 2005.
- [24] S. Rezaee, E. Farjah, and B. Khorramdel, "Probabilistic analysis of plug-in electric vehicles impact on electrical grid through homes and parking lots," *IEEE Trans. Sustain. Energy*, vol. 4, no. 4, pp. 1024–1033, Oct. 2013.
- [25] E. Wikner and T. Thiringer, "Extending battery lifetime by avoiding high SOC," *Appl. Sci.*, vol. 8, no. 10, pp. 1–16, 2018.
- [26] S. Rezaee, E. Farjah, and B. Khorramdel, "Probabilistic analysis of plug-in electric vehicles impact on electrical grid through homes and parking lots," *IEEE Trans. Sustain. Energy*, vol. 4, no. 4, pp. 1024–1033, Oct. 2013.
- [27] A. Aktel, B. Yagmahan, T. Özcan, M. M. Yenisey, and E. Sansarci, "The comparison of the metaheuristic algorithms performances on airport gate assignment problem," *Transp. Res. Procedia*, vol. 22, pp. 469–478, Jan. 2017.
- [28] J. Schrieber, D. Schuhmacher, and C. Gottschlich, "DOTmark—A benchmark for discrete optimal transport," *IEEE Access*, vol. 5, pp. 271–282, 2016.
- [29] N. Shlayan, K. Challapali, D. Cavalcanti, T. Oliveira, and Y. Yang, "A novel illuminance control strategy for roadway lighting based on greenshields macroscopic traffic model," *IEEE Photon. J.*, vol. 10, no. 1, Feb. 2018, Art. no. 8200211.
- [30] F. A. Hashim, E. H. Houssein, M. S. Mabrouk, W. Al-Atabany, and S. Mirjalili, "Henry gas solubility optimization: A novel physics-based algorithm," *Future Gener. Comput. Syst.*, vol. 101, pp. 646–667, Dec. 2019.
- [31] N. G. Omran and S. Filizadeh, "Location-based forecasting of vehicular charging load on the distribution system," *IEEE Trans. Smart Grid*, vol. 5, no. 2, pp. 632–641, Mar. 2014.
- [32] Specifications of Tesla Roadster, 2020. [Online]. Available: <https://www.tesla.com/roadster>
- [33] Specifications of BMW EVs, 2020. [Online]. Available: <https://www.bmwusa.com/vehicles/bmw.html>
- [34] Z. Liu, E. Blasch, and V. John, "Statistical comparison of image fusion algorithms: Recommendations," *Inf. Fusion*, vol. 36, pp. 251–260, 2017.



Sourav Das (Student Member, IEEE) received the B.Tech. degree in electrical engineering from the Maulana Abul Kalam University of Technology, West Bengal (formerly known as West Bengal University of Technology), Kolkata, India, in 2016, and the M.Tech. degree in electrical power system from the National Institute of Technology Durgapur, Durgapur, India, in 2018, where he is currently working toward the Ph.D. degree in electrical engineering.

His current research interest include power system optimization, and renewables and electric Vehicle.



Parimal Acharjee (Senior Member, IEEE) received the B.E.E. degree from the University of North Bengal, Siliguri, India, in 1996, and the M.E.E. and Ph.D. degrees in electrical power system from Jadavpur University, Kolkata, India, in 2001 and 2007, respectively.

He has three years of industrial experience and 15 years of teaching experience. He is currently with the National Institute of Technology Durgapur, Durgapur, India, as an Associate Professor. His current research interest is the application of soft computing techniques in various power system problems, flexible ac transmission system devices, smart grid, distributed generation, and phasor measurement unit.

Dr. Acharjee was a recipient of the Indo-U.S. Research Fellowship.



Aniruddha Bhattacharya (Member, IEEE) received the B.Sc. Eng. degree in electrical engineering from the National Institute of Technology, Jamshedpur, Jamshedpur, India, in 2000, and the M.E.E. and Ph.D. degrees in electrical power system from Jadavpur University, Kolkata, India, in 2008 and 2011, respectively.

His employment experience include Siemens Metering Limited, India; Jindal Steel and Power Limited, Raigarh, India; Bankura Unnyani Institute of Engineering, Bankura, India; Dr. B. C. Roy Engineering College, Durgapur, India; National Institute of Technology Agartala, India. He is currently an Assistant Professor with Electrical Engineering Department, National Institute of Technology Durgapur, Durgapur, India. His areas of interest include power system optimal power flow, hydrothermal scheduling, power system stability, power system optimization, and electric vehicle.